Photodiagnosis and Photodynamic Therapy 27 (2019) 380–384

Contents lists available at ScienceDirect

Photodiagnosis and Photodynamic Therapy

journal homepage: www.elsevier.com/locate/pdpdt

Potential colorimetric detection of cancer cells using Phenol Red

Erny Nurliessa Amran[a], Suhainah Sudik[a], Ahmad Fairuz Omar[a,*], Mohd Hafiz Mail[b,c], Azman Seeni[b,c]

[a] School of Physics, Universiti Sains Malaysia, 11800, Penang, Malaysia
[b] Malaysian Institute of Pharmaceuticals and Nutraceuticals, National Institute of Biotechnology Malaysia, Ministry of Energy, Science, Technology, Environment and Climate Change, 11700, Penang, Malaysia
[c] Advanced Medical and Dental Institute, Universiti Sains Malaysia, Bertam, 13200, Pulau Pinang, Malaysia

ARTICLE INFO

Keywords:
DU145
HeLa
L929
pH
Phenol Red
Visible absorbance spectroscopy
colorimetric detection

ABSTRACT

The objective of this research is to examine the relationship between the color changes of phenol red and the growth of cancer cells, i.e., HeLa and DU145 cells, over a specific period of time. Normal mouse skin fibroblasts (L929 cells) were used as a reference. In this research, the color changes of phenol red due to the acidification of the cell culture medium from the growth of the cells over a period of nine hours showed potential colorimetric characteristics of cancer cells. The color changes of phenol red were observed using visible absorbance spectroscopy. The transformation of the absorbance spectra into coefficients of determination against the examined range of wavelengths created a distinctive spectral signature that signifies phenol red discoloration in cancer and normal cell culture lines.

1. Introduction

The ideal pH for most cultured cells is approximately 7.4 [1]. However, cellular respiration produces carbon dioxide and lactate, which can acidify the culture medium over time. This process can significantly alter the microenvironment of the cells due to the small volume of the growth medium [2]. Cancer cells, on the other hand, cater to their uncontrolled proliferation, require energy metabolism to fuel cell division and tumor growth [3] and thus exhibit high rates of glycolysis that lead to the production of high amounts of lactate; as a result, their environment is acidified [4–6]. In addition, electrode-based pH measurements between human tumors and adjacent normal tissues are considerably and consistently lower in tumors than in normal tissues. This observation is believed to mainly represent tissue extracellular pH [7]. The intracellular pH (pHi) in normal differentiated adult cells is approximately 7.2, which is lower than the extracellular pH (pHe), which is approximately 7.4. However, compared to normal cells, cancer cells have a high pHi of above 7.4 and a low pHe of approximately between 6.7 and 7.1 [8,9].

Phenol red is a common pH indicator that is available within most commercial cell culture media to monitor the cellular environment. Phenol red changes color depending on the pH level [2]. Phenol red has been used in various colorimetric applications, such as the examination of freshwater pH [10], the diagnosis of filarial infection [11], and the measurement of hydrogen peroxide produced by cells in culture [12] and carbon dioxide pressure in carbonated liquids [13]. Phenol red has also been applied in assisting biopsy procedures to determine *Helicobacter pylori*-infected areas for patients with early gastric cancers [14].

In this paper, the relationship between the color changes of phenol red and the pH of the cell culture medium is used to determine the progression of cells over 9 h and the potential of this method to differentiate between normal and cancerous cells. This research used human cervix adenocarcinoma cells, HeLa and human prostate carcinoma DU145 cells and mouse skin fibroblast L929 cells, with normal cells as reference.

2. Materials and methods

Three different cell lines were used in this study: mouse skin fibroblast L929 cells, human cervix adenocarcinoma cells, and HeLa and human prostate carcinoma DU145 cells. These cell lines were purchased from American Tissue Culture Collection (ATCC), Manassas, VA, USA. The L929 and DU145 cells were cultured in minimum essential medium (MEM), whereas the HeLa cells were cultured in Dulbecco's modified Eagle medium (DMEM). All culture media were supplemented with 10% fetal bovine serum (FBS), 1 mM sodium pyruvate, 100 U/mL penicillin and 100 µg/streptomycin. The cell cultures were maintained at 37 °C in a humidified atmosphere incubator containing 5% CO_2 and

* Corresponding author.
E-mail address: fairuz_omar@usm.my (A.F. Omar).

https://doi.org/10.1016/j.pdpdt.2019.07.006
Received 9 March 2019; Received in revised form 23 May 2019; Accepted 8 July 2019
Available online 10 July 2019
1572-1000/

Table 1
Total numbers of cells seeded.

Cell Line	Initial culture concentration (cells/ml)	Seeded cell concentration (cells/ml)	Seeded cells per well
L929	1,925,000	25,025	75,075
HeLa	2,105,000	24,558	73,675
DU145	820,000	24,873	74,620

95% air. The concentration of cells was initially determined using a hemocytometer before dilution to give uniform total cell numbers and concentrations when seeded into 6-well plates (3 ml volume of media per cell). The initial cell culture concentrations and diluted cell numbers and concentrations are given in Table 1.

The growth rate can be measured from the cell population doubling time, the time required for a culture to double in number. The doubling times for L929, HeLa and DU145 were 24, 18 and 40 h, respectively. Based on the seeding number and doubling time, the estimated total cell number after 9 h of incubation (total incubation period was 33 h, including 24 h for incubating the seeded cells) were 194744, 262577, and 132152 for the L929, HeLa and DU145 cells, respectively. The calculation formula is represented by Eq. 1:

$$Xe = e^{\left(T\frac{ln2}{DT}\right)}Xb \quad (1)$$

where DT is the doubling time

T is the incubation time

Xb is the cell seeding number

and Xe is the cell number at the end of the incubation period

The wells were replaced with fresh media prior to the spectroscopy measurement. Fig. 1 illustrates the experimental setup for the visible absorbance spectroscopy measurement of the (a) cultured cell lines and (b) control samples (free of cells). The absorbance measurement of the cultured cell lines was calibrated using an empty well. The spectroscopy instruments used in this experiment are from Ocean Optics Inc. (Dunedin, Florida, USA). Prior to the spectroscopy measurement, another 5% FBS was added to all samples to increase the growth rate of the cells, which were then kept for one hour in the incubator at 37 °C, humidified with 5% CO_2 and 95% air. The illumination light source was connected to a tungsten halogen light source, HL-2000, with a range of emission wavelengths between 360 and 2400 nm and a color temperature of 2800 K. The resultant light from the interaction with the sample transmitted through the well was collected using a retrieving fiber. The fiber was connected to a QE65000 spectrometer with a spectral sensitivity between 400 and 1050 nm. However, the entire analysis only utilized visible wavelengths between 400 and 600 nm. The acquisition parameters for the spectrometer were set as follows: integration time = 17 ms, scan to average = 8, and boxcar width = 3.

Three wells used on each plate contained the same cell type. The absorbance in each well was measured three times every hour, starting from the first hour after the samples were prepared until 9 h. In addition, the microscopy images of the cells were captured using an inverted microscope at 100 times magnification (Olympus model CKX41SF) to observe the morphology and distribution of cells over time. The original color of the cultured cell lines is bright pink.

The control samples only contained medium without cells and were prepared in a 6-well plate before they were placed in the incubator under similar conditions and time frames as those of the cultured cell lines prior to the absorbance spectroscopy measurement. The medium was prepared in 9 different wells, and the sample from each well was extracted every hour and placed in a quartz cuvette for the absorbance measurement.

3. Results and analysis

The coefficient of determination, R^2, is generally used as a parameter to define the accuracy of a developed model. In this research, R^2 was used as a tool to determine the visible spectral response, i.e., the color changes of phenol red as the cells gradually grew over 9 h of experiment, to evaluate the potential spectral signature that can be used to distinguish between normal and cancerous cells.

The absorbance measurement was conducted on control samples as a reference to the generated spectral signatures for the cultured normal and cancerous cell lines. Fig. 2 (a) shows the visible spectral absorbance of control samples that contain only medium and phenol red (free of cells) with distinctive pH values between 8.1 and 7.62 after 9 h of incubation. The spectrum at pH 8.1 represents the original acidity of the medium, while the others are the result of color changes of phenol red due to gradual acidification by the CO_2 in the incubator. Fig. 2 (b) shows the linear relationship and direct proportionality between the absorbance at 557 nm and the pH of phenol red, which generated a very high coefficient of determination (R^2) of 0.9892. Fig. 2 (c) shows the spectral signature graph of phenol red based on the relationship between the computed coefficient of determination and wavelengths between 400 and 600 nm. From the graph, high linearity can be observed between absorbance and pH for wavelengths between 510 and 580 nm with an R^2 value above 0.97 and a peak response at 557 nm. The

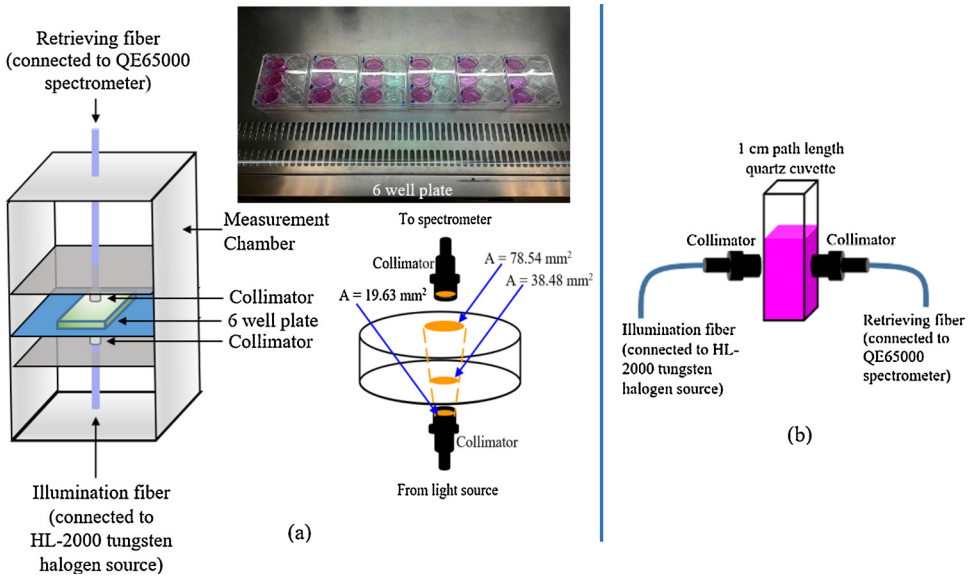

Fig. 1. Experimental setups for the visible absorbance spectroscopy measurement: (a) The absorbance measurement of the cultured cell lines (i.e., L929, HeLa and DU145) through a custom-made chamber. Three wells used on each plate contained the same cell type. Two sets of similar cell lines were prepared: one set for the absorbance spectroscopy measurement while the other set for image analysis. An illustration of the light divergence toward the well and the effective area covered by the illuminated light is also shown in the figure. (b) Simplified illustration of typical absorbance spectroscopy measurements conducted on control samples (free of cells) through a quartz cuvette with a 1 cm path length.

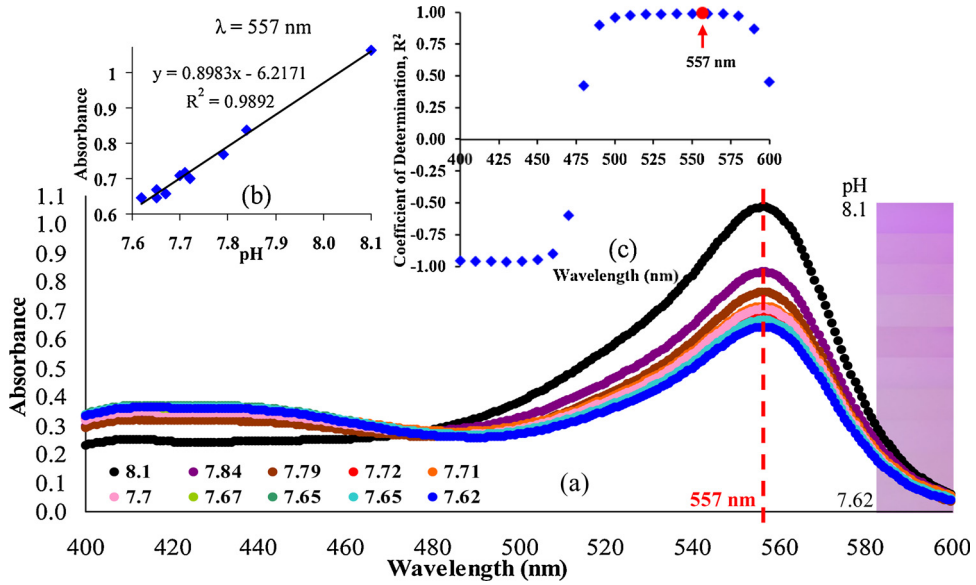

Fig. 2. (a) Visible absorbance spectra of phenol red under different pH levels. (b) Linear regression between absorbance and pH at a wavelength of 557 nm. (c) Graph of the coefficient determination R^2 versus wavelength (nm). The red data point represents the highest value of R^2 recorded at a wavelength of 557 nm.

absorbance and pH values are directly proportional to each other for wavelengths between 480 and 600 nm, and a positive R^2 is noted in the graph. However, for wavelengths between 400 and 470 nm, the relationship between absorbance and pH reverts to inversely proportional and is noted as a negative R^2 in the graph. The direct proportionality and inverse relationship between the absorbance and pH at different regions in the visible spectra is due to the color transformation of phenol red from the reduction in its original bright pink color to the slight increment in the orange appearance of the medium.

The color changes of the samples due to the growth of the cells over time were also directly attributed to phenol red and are represented by the visible absorbance spectroscopy data between 400 and 600 nm. The color changes of phenol red can be attributed to the gradual acidification of the medium by the cells and their subsequent growth in the medium over the period of nine hours. Fig. 3 (a), (b) and (c) shows the absorbance graph for the cultured L929, HeLa and DU145 cells, respectively. The major peak absorbance is located at 557 nm for all measured spectra, similar to that of the control samples. The secondary peak is located at 407 nm. The highest spectral peak was recorded for the HeLa cell line with absorbance at 0.355, followed by that for DU145 with absorbance at 0.291 and that for normal mouse skin fibroblasts, L929, with absorbance at 0.243. The spectra show a general increase in absorbance at longer time points. This increase could be a result of the continuous cell growth over time within the single well. However, throughout the duration of the experiment, the color of phenol red changes from bright pink to light pink. Hence, the spectral response

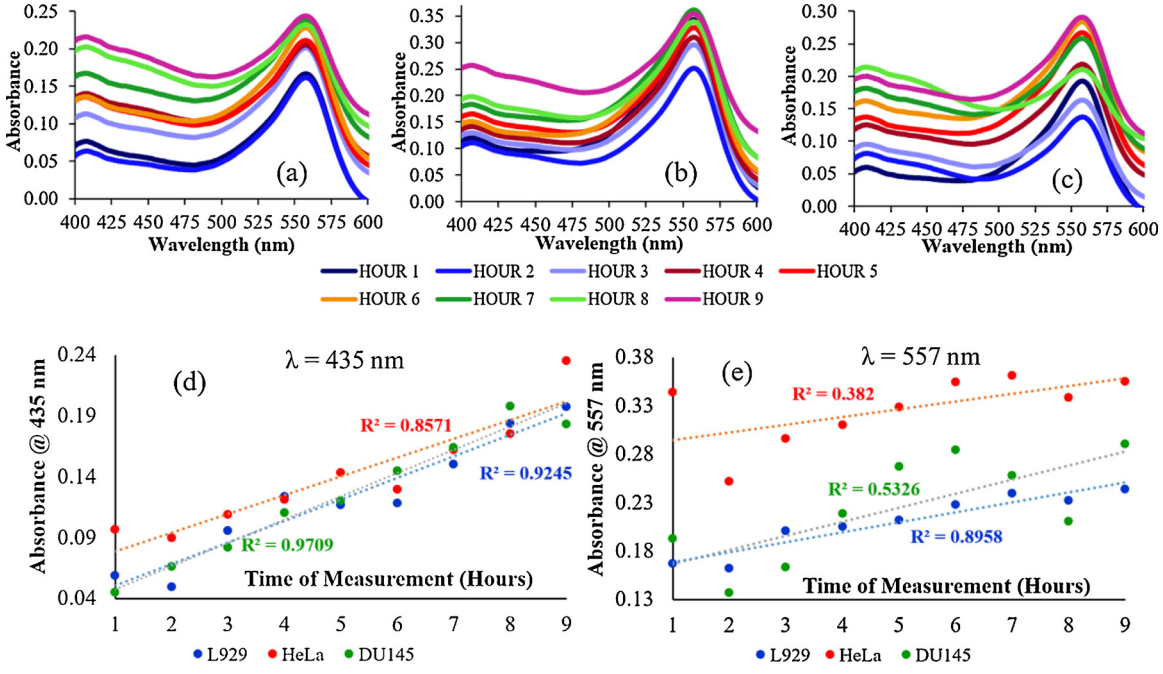

Fig. 3. Absorbance versus wavelength data for (a) normal cells, (b) cervical cancer cells, and (c) prostate cancer cells collected for nine hours. The absorbance spectra are the averaged values from all three wells (per plate for the same cell type). The linear regression was generated between the absorbance and time of measurement at (c) 435 nm and (d) 557 nm.

may not be entirely due to the absorption by phenol red because the relationship between absorbance and time would be expected to be inversely proportional, especially at the peak absorbance wavelength. As a comparison, the response of the control samples (Fig. 2 (b)) shows a direct proportionality between absorbance and pH or a supposedly inverse relationship with time (hours) for the experiment with the cultured cell line. Notably, from the spectroscopy experimental setup, the value of absorbance represents the total attenuation of light through the samples as a result of light absorption mainly by the color of the medium and the light scattering by the cells.

Fig. 3 (d–e) shows the relationship between absorbance and time of measurement for two distinctive wavelengths: 557 nm, which is the peak absorbance wavelength, and 435 nm, which is the wavelength that produced the higher R^2. Comparatively, for all types of cells, R^2 generated at the peak absorbance wavelength is much lower than that at 22 nm away from the peak. This finding is particularly obvious for the cancer cell lines. For instance, the relationship between the absorbance of the HeLa cells and the time of measurement only generated an R^2 of 0.382 at 557 nm and was capable of generating a higher R^2 of 0.8571 at 435 nm. This result indicates that the scattering of light by the steady growth of cells over the experimental period is strongly proportional with the time of measurement. While the light absorption by phenol red was expected to gradually decrease over a similar experimental period, the resultant absorbance (i.e., absorption α 1 / time & scattering α time) at the peak of the spectra shall distort the final values of R^2.

Fig. 4 shows the values of R^2 produced for wavelengths between 400 and 600 nm with 5 nm gaps. As expected, the peak absorbance for the samples produced the lowest R^2; however, when the wavelength is located beyond the peak toward the shoulders of the curve, the R^2 values are much higher and considerably constant. This observation is in contrast with the signature obtained from the control samples (Fig. 2 (c)), where the peak R^2 value is located at a similar wavelength as that for the peak absorbance, thus strengthening the hypothesis of the role of light scattering by the cells in the development of spectral signatures. Furthermore, the signature in Fig. 2 does not portray sharp differences between the peak response at 557 nm and its neighboring wavelengths primarily because of the low amount of significant color changes in phenol red, which occur only due to minimal acidification by CO_2, compared to those color changes in the cultured cells, particularly the cancer cells.

Fig. 4 (a) shows the response from all 3 wells in the 6-well plate that were prepared to initially contain a similar number of cells. From the graph, phenol red in the L929 cells displays high consistency in reproducing the values of R^2 through its color changes across the examined spectrum compared to that in the HeLa and DU145 cells. The range of R^2 observed for L929 was between 0.866 and 0.833 at 555 nm, while the range of R^2 was between 0.426 and 0.181 for HeLa and between 0.622 and 0.426 for DU145 at similar wavelengths. Fig. 4 (b) shows the averaged signature for the cells. The graph illustrates obvious differences between the spectral signatures of normal L929 cells and cancerous HeLa and DU145 cells due to the rapid discoloration of phenol red for HeLa and DU145.

Fig. 5 shows the morphological difference between the normal cells, cervical cancer cells and prostate cancer cells during one, five and nine hours of measurement. In the image, there are changes in the number of cells from the first hour of the experiment until the ninth hour as the number of cells gradually increased in the medium. The growth of the prostate cancer cells appears to be slow from the image obtained. The increase in the number of cells contributes to the increase in the light scattering that leads to the increment in the measured absorbance of the sample. The scattering signal may be attributed to the nucleus, which is often the largest organelle in the cell, and cytoplasmic organelles, including mitochondria, lysosomes and peroxisomes, or may be produced by all portions of the cell [15,16]. The variability in subcellular sources of scattering may be due to the morphology and measurement conditions of the cell [16]. In addition, cancer cells have larger nuclei and more variation in nuclear size than do normal cells [17]. The light scattering by the cells explains the high R^2 value produced beyond the peak absorbance wavelength of phenol red, as shown in Fig. 3.

In summary, the ability of phenol red to change its color due to the alteration of the pH level in the cultured cell medium can be used as a potential colorimetric indicator for cancer cells. Analysis of nine continuous hours of visible absorbance spectroscopy data for the cultured cancer cells, i.e., HeLa and DU145, with phenol red exhibit distinctive signatures compared to those for the normal L929 cells. The major changes in the phenol red color from bright pink to light pink can be attributed to the acidification of the culture medium by the cells and is accelerated for the cancer cells. This finding demonstrates the promising application of phenol red in cancer detection. Further research is needed to examine the potential of phenol red to assist in the identification of the interface between cancer and normal tissue, which may be great assistance during surgical biopsy in the total removal of cancer cells.

Author contributions

A.F.O and A.S. designed the research study. E.N.A, A.F.O and M.H.M performed the experiments. A.F.O, E.N.A and S.S. analysed data from the experiments. A.F.O and M.H.M wrote the paper. A.S. and M.H.M edited and finalised the paper.

Funding

This research received no external funding.

Declaration of competing interest

The authors declare no conflict of interest.

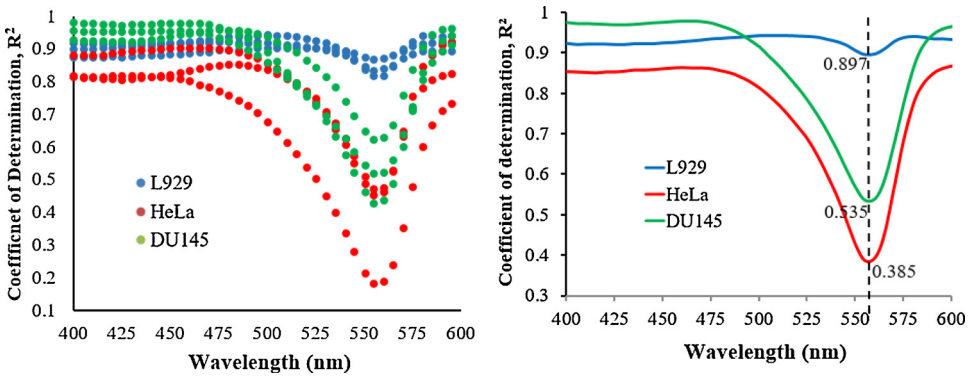

Fig. 4. (a) Coefficient of determination versus wavelength for cultured L929, HeLa and DU145 cells during nine hours of visible absorbance measurement. The graph shows the response from all three wells and (b) the average response from Fig. 3 (a).

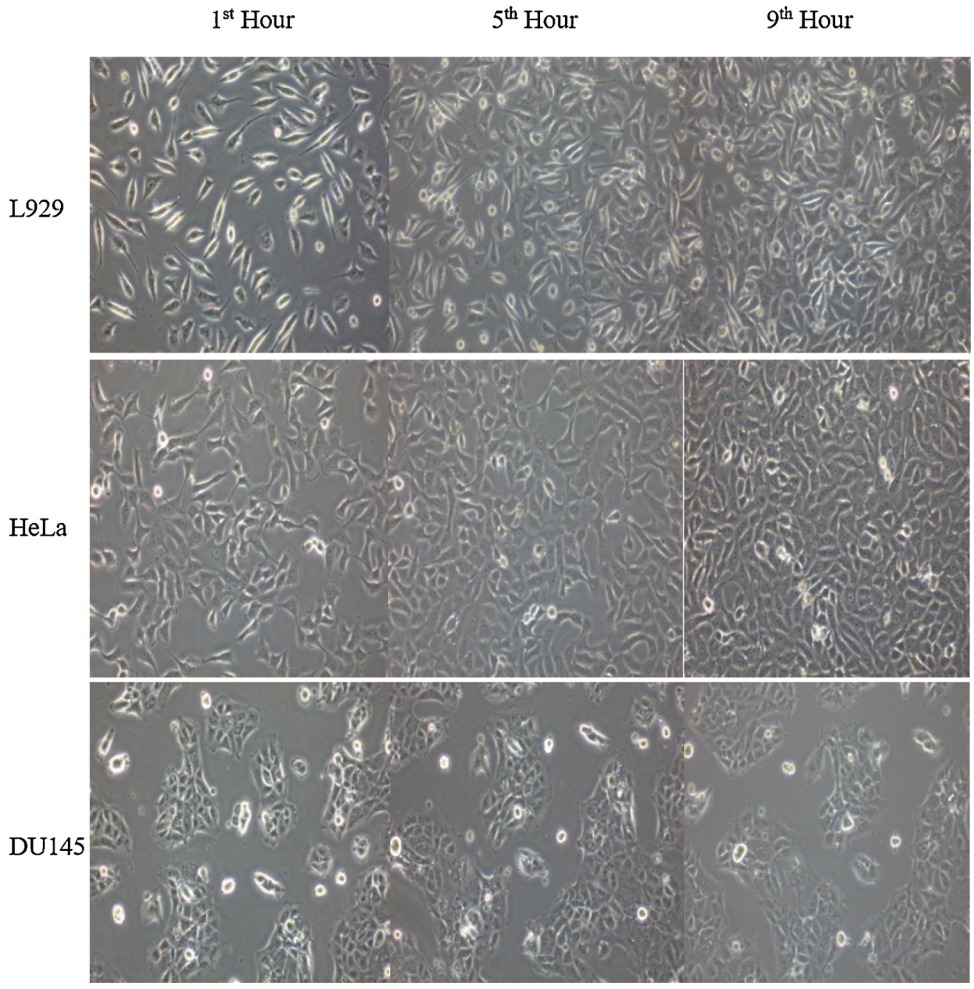

Fig. 5. Morphology of normal cells, cervical cancer cells and prostate cancer cells during the first hour, the next five hours and the next nine hours of measurement using 100 times magnification under an inverted microscope.

Acknowledgments

This experiment was conducted in Integrative Medicine Cluster, Advanced Medical and Dental Institute (AMDI) Universiti Sains Malaysia, Kepala Batas, Pulau Pinang.

References

[1] R.I. Freshney, Culture of Animal Cells: a Manual of Basic Technique and Specialized Applications, John Wiley & Sons, 2015.
[2] E.B. Magnusson, S. Halldorsson, R.M. Fleming, K. Leosson, Real-time optical pH measurement in a standard microfluidic cell culture system, Biomed. Opt. Express 4 (9) (2013) 1749–1758.
[3] D. Hanahan, R.A. Weinberg, Hallmarks of cancer: the next generation, cell 144 (5) (2011) 646–674.
[4] R.A. Gatenby, R.J. Gillies, Why do cancers have high aerobic glycolysis? Nat. Rev. Cancer 4 (11) (2004) 891.
[5] S. Granja, D. Tavares-Valente, O. Queiros, F. Baltazar, April). Value of pH Regulators in the Diagnosis, Prognosis and Treatment of Cancer. In Seminars in Cancer Biology Vol. 43 Academic Press, 2017, pp. 17–34.
[6] Institute for Research in Biomedicine (IRB Barcelona), July 31). Acidic pH: the Weakness of Cancer Cells. ScienceDaily, Retrieved February 7, 2019 from (2018) www.sciencedaily.com/releases/2018/07/180731104216.htm.
[7] L.E. Gerweck, K. Seetharaman, Cellular pH gradient in tumor versus normal tissue: potential exploitation for the treatment of cancer, Cancer Res. 56 (6) (1996) 1194–1198.
[8] B.A. Webb, M. Chimenti, M.P. Jacobson, D.L. Barber, Dysregulated pH: a perfect storm for cancer progression, Nat. Rev. Cancer 11 (9) (2011) 671.
[9] E. Persi, M. Duran-Frigola, M. Damaghi, W.R. Roush, P. Aloy, J.L. Cleveland, et al., Systems analysis of intracellular pH vulnerabilities for cancer therapy, Nat. Commun. 9 (1) (2018) 2997.
[10] C.Z. Lai, M.D. DeGrandpre, B.D. Wasser, T.A. Brandon, D.S. Clucas, E.J. Jaqueth, et al., Spectrophotometric measurement of freshwater pH with purified meta-cresol purple and phenol red, Limnol. Oceanogr. Methods 14 (12) (2016) 864–873.
[11] C.B. Poole, Z. Li, A. Alhassan, D. Guelig, S. Diesburg, N.A. Tanner, et al., Colorimetric tests for diagnosis of filarial infection and vector surveillance using non-instrumented nucleic acid loop-mediated isothermal amplification (NINA-LAMP), PLoS One 12 (2) (2017) e0169011.
[12] E. Pick, Y. Keisari, A simple colorimetric method for the measurement of hydrogen peroxide produced by cells in culture, J. Immunol. Methods 38 (1-2) (1980) 161–170.
[13] A. Mills, G.A. Skinner, A novel 'fizziness' indicator, Analyst 136 (5) (2011) 894–896.
[14] K. Iseki, M. Tatsuta, H. Iishi, M. Baba, S. Ishiguro, Helicobacter pylori infection in patients with early gastric cancer by the endoscopic phenol red test, Gut 42 (1) (1998) 20–23.
[15] R. Drezek, A. Dunn, R. Richards-Kortum, Light scattering from cells: finite-difference time-domain simulations and goniometric measurements, Appl. Opt. 38 (16) (1999) 3651–3661.
[16] R.A. Drezek, M. Guillaud, T.G. Collier, I. Boiko, A. Malpica, C.E. MacAulay, et al., Light scattering from cervical cells throughout neoplastic progression: influence of nuclear morphology, DNA content, and chromatin texture, J. Biomed. Opt. 8 (1) (2003) 7–17.
[17] A. Burton, Light for lightening diagnoses, Lancet Oncol. 3 (5) (2002) 264.